Limnol. Oceanogr., 53(2), 2008, 494–505

Acclimation to elevated carbon dioxide and ultraviolet radiation in the diatom *Thalassiosira pseudonana*: Effects on growth, photosynthesis, and spectral sensitivity of photoinhibition

Cristina Sobrino,[1] *Mary Love Ward, and Patrick J. Neale*
Smithsonian Environmental Research Center, Edgewater, Maryland 21037

Abstract

We studied the effects of elevated CO_2 concentrations (0.03% vs. 0.1%) on light absorption, membrane permeability, growth, and carbon fixation under photosynthetically active radiation (PAR) and ultraviolet radiation (UVR) exposures in the diatom *Thalassiosira pseudonana*. Susceptibility of photosynthesis to UVR was estimated using biological weighting functions (BWFs) for the inhibition of photosynthesis and a model that predicts primary productivity under PAR and UVR exposures. Elevated CO_2 concentrations reduced chlorophyll content and increased chlorophyll specific cross section, carbon fixation per chlorophyll, and growth rates. In addition, cells acclimated to high CO_2 were more sensitive to photoinhibitory UVR than those under atmospheric levels. Sensitivity to UVR was also related to the growth light regime; despite the fact that no UVR effects were observed on growth, light absorption, or carbon fixation, cells pre-exposed to UVR showed reduced photoinhibition compared to those grown under PAR for both normal and elevated CO_2 cultures. Thus, acclimation to UVR partially counteracted the increased susceptibility observed under elevated CO_2 conditions.

Anthropogenic activities that influence the global environment are mainly those that affect the atmosphere, resulting in, for example, increased exposures to ultraviolet radiation (UVR; 280–400 nm) and higher CO_2 levels. The effects of these changes are propagated to aquatic systems through the surface layer (Sabine et al. 2004), where most of the biological processes that sustain life and biogeochemical processes take place. Phytoplankton play a key role in determining the effects of environmental change on the surface layer since they are responsible for dissolved inorganic carbon (DIC) sequestration through photosynthetic processes.

CO_2 used for photosynthesis can diffuse through the cell membrane of most phytoplankton species, while both CO_2 and HCO_3^- can be incorporated through adenosine triphosphate (ATP)-dependent mechanisms called CO_2 concentrating mechanisms (CCMs) (reviewed by Raven 1997). It is expected that long-term elevation of CO_2 would downregulate the activity of CCMs, increasing the energy available for other cellular processes and resulting in increased carbon fixation and growth rates (Raven 1991). However, the effect of elevated CO_2 on growth and photosynthesis differs among studies, and more work is still needed to understand phytoplankton response to a rise in CO_2 concentrations (Riebesell et al. 1993; Hein and Sand-Jensen 1997; Tortell et al. 2000). A proper evaluation of future CO_2 concentrations depends not only on estimates of the carbon emitted from anthropogenic activities and stored in the atmosphere, but also on our knowledge of the physical and biological processes affecting ocean–atmosphere feedback. Recent results have suggested that variation among experiments can be related to both interspecific differences in the mechanisms responsible for carbon incorporation as well as the dependence of biological DIC uptake on other factors, such as nutrients and light availability (Leonardos and Geider 2005).

Exposure to UVR is one of the environmental factors that can modify atmospheric CO_2 sequestration by phytoplankton. Short wavelengths of solar radiation below 400 nm have enough energy to break molecular bonds and damage phytoplankton cells (reviewed in Vincent and Neale 2000). UVR can also indirectly affect several targets in the cells through oxidative stress. Among these cellular targets, cell membranes can be damaged by UVR through lipid peroxidation, cell wall degradation, or protein channel inhibition (Murphy 1983; Sobrino et al. 2004). Membrane damage might also increase permeability, facilitating CO_2 diffusion, but it is unlikely that any benefit from an increase in passive CO_2 flux could counteract the UVR damage in cells with compromised membranes. Excessive UVR damage of the membrane can also depress the nitrate and phosphorus uptake mechanisms (Hessen et al. 1995; Sobrino et al. 2004). The specific effect of UV exposure on CCMs is unknown, but effects could be caused by nonspecific damage to deoxyribonucleic acid (DNA), gene transcription machinery, or direct damage to membrane-protein complexes. In fact, a study analyzing the photoinhibitory effect of UVR on inorganic carbon acquisition by *Dunaliella tertiolecta* showed that carbon incorporation did not change after short-term exposures to UVB (280–320 nm) in this species (Beardall et al. 2002).

As an overall effect of UVR damage on phytoplankton, it has been reported that exposure to UVR decreases primary productivity and biomass in many regions of

[1] Present address: Universidade de Vigo, 36310 Vigo, Pontevedra, Spain.

Acknowledgments

We appreciate the helpful comments of two anonymous reviewers. This research was supported by the Spanish Ministry of Education and Science and the Smithsonian Institution through postdoctoral fellowship to C.S. and internship to M.L.W. Additional support was also obtained from the U.S. National Science Foundation, Ecosystems and Polar Programs.

oceans, lakes, and estuaries (Neale et al. 1998; Banaszak and Neale 2001; Leavitt et al. 2003). The opposing effects of UVR and CO_2 on phytoplankton have led to the proposition that the increase in UVB caused by the reduction of the ozone layer could act as a negative feedback to the enhancement of productivity due to increased atmospheric CO_2 (Williamson and Platt 1991). Although the chlorine concentration in the stratosphere has recently leveled off, reflecting the implementation of the Montreal Protocol, the time needed for recovery of the ozone layer is uncertain and will depend on the effects of climate change on the stratosphere (Weatherhead and Andersen 2006). Predictions for responses to UVR exposure are complex because several factors, such as the spectral composition or the light acclimation history, among others, can interact, affecting phytoplankton sensitivity to UVR (Neale 2001; Villafañe et al. 2004; Litchman and Neale 2005). Most of the UVR effects in natural samples have been attributed to the UVA region (320–400 nm) (Villafañe et al. 2004). Nevertheless, an assessment of the response to harmful short wavelengths in the UVB range remains important due to their dependence on stratospheric ozone concentrations. In addition, it has been observed that phytoplankton from turbid waters or acclimated to low-light conditions are more sensitive to UVR than those from clear waters (Villafañe et al. 2004; Litchman and Neale 2005). Estimation of the sensitivity to UVR exposure in relation to wavelength can be quantified by biological weighting functions (BWFs) (reviewed by Neale 2000). They allow comparison between responses to different spectral UVR conditions and can be utilized to predict effects if applied using an appropriate model. Assessments of photosynthetic rates under UVR that combine BWFs for the inhibition of phytoplankton photosynthesis with primary productivity models have shown tenfold variations in the sensitivity of phytoplankton photosynthesis to UVR, and decreases of 16% to 30% in areal primary productivity of lakes, estuarine, and Antarctic waters (Gala and Giesy 1991; Boucher and Prézelin 1996; Neale 2001). Recent results have shown that sensitivity to UVR can also change depending on the external CO_2 concentrations. Sobrino et al. (2005) demonstrated that two picoplanktonic marine species with similar morphology but different CCMs showed different responses to increased CO_2 levels: *Nannochloropsis gaditana*, a species that relies on bicarbonate uptake for photosynthesis, decreased sensitivity to UVA after growing 4 d under elevated CO_2 conditions. In contrast, *Nannochloris atomus*, a species with a CO_2 active transport, showed similar sensitivity to UVR with and without supplemental CO_2. These studies did not verify the potential effect of UVR on CCMs but showed that differences in UVR sensitivity related to external CO_2 concentrations can affect taxonomic composition in algal communities. Despite the relevance of these findings to aquatic primary productivity and carbon budgets, studies of the effects of UVR on processes related to carbon incorporation metabolism are scarce (Beardall et al. 2002; Sobrino et al. 2005).

Among the phytoplankton species inhabiting the surface layer, diatoms are responsible for almost 40% of the ocean primary productivity (Nelson et al. 1995). The objective of this study was to analyze the interactive effects of increased CO_2 and UVR in a widely distributed diatom, *Thalassiosira pseudonana*, grown under different light regimes combining photosynthetically active radiation (PAR; 400–700 nm) and UVR exposures. *T. pseudonana* can incorporate Ci directly as HCO_3^- (Elzenga et al. 2000). Key enzymes of the C4 photosynthetic pathway occur in its genome, suggesting that a C4-based CCM can operate in some diatoms (Reinfelder et al. 2000), but many aspects still need clarification (Armbrust et al. 2004; Granum et al. 2005). Our results show the effects of UVR and CO_2 on membrane permeability, light absorption, growth, and photosynthetic parameters as well as variations in the spectral response of *T. pseudonana* sensitivity of photosynthesis to UVR.

Materials and methods

Culture growth conditions—Thalassiosira pseudonana (Husted) Hasle and Heimdal, *Bacillariophyceae* was provided by the Provasoli–Guillard Center for Culture of Marine Phytoplankton, Maine, USA (CCMP1335, strain 3H). Cultures were grown in 500-mL UVR-transparent Teflon bottles (PTFE) at 20°C using a semicontinuous approach through daily dilutions with fresh growth medium. The growth medium was filtered seawater from the Gulf Stream that was adjusted to a salinity of 15 and enriched with f/2 nutrients. The cultures were continuously aerated using 0.2-μm filtered air containing two different CO_2 partial pressures in the medium: (1) atmospheric CO_2: cultures aerated with regular levels of CO_2 (38.50 Pa = 380 ppmv CO_2 = 0.038% CO_2); and (2) elevated CO_2: cultures aerated with air containing 0.1% CO_2 (101.3 Pa = 1,000 ppmv CO_2, which mimics maximum CO_2 levels estimated for the end of the century [IPCC 2001]). The 0.1% CO_2 tank was provided by Airgas Co. Aeration with 0.1% CO_2 changed the pH of the media from 8.1 to 7.5 $\pm$ 0.1. Cultures were illuminated with 250 μmol photons m^{-2} s^{-1} PAR irradiance (54.3 W m^{-2} applying a 4.6 μmol quanta J^{-1} conversion factor) provided by cool-white fluorescent lamps and following a 14 : 10 light : dark (LD) photoperiod. PAR scalar irradiance was measured inside a Teflon bottle filled with filtered seawater using a 4-π PAR sensor, QSL-2101 (Biospherical Instruments Inc.). Additional UVR was provided by UVA-340 lamps (Q-lab Corp.). For the PAR light treatment, the Teflon bottles were wrapped with COURTGARD™ clear UV-absorbing film (CPFilm), which removes most of the UVR and allows the transmission of PAR (nominal 50% transmittance [T] at 400 nm). For the UVR treatment, bottles were wrapped with cellulose acetate film (Ref. 8564K, McMaster-Carr Supply Co.), which removes the short wavelengths of the UVB range (nominal 50% transmittance [T] at 295 nm) and allows the transmission of most UVR and PAR. PAR fluorescent lamps were placed above and below the flasks, and the UVR lamps were situated vertically in the growth chamber. To mimic natural conditions, UVR exposure was applied during a 6-h interval centered in the middle of the PAR light period. UVR and PAR spectral irradiance

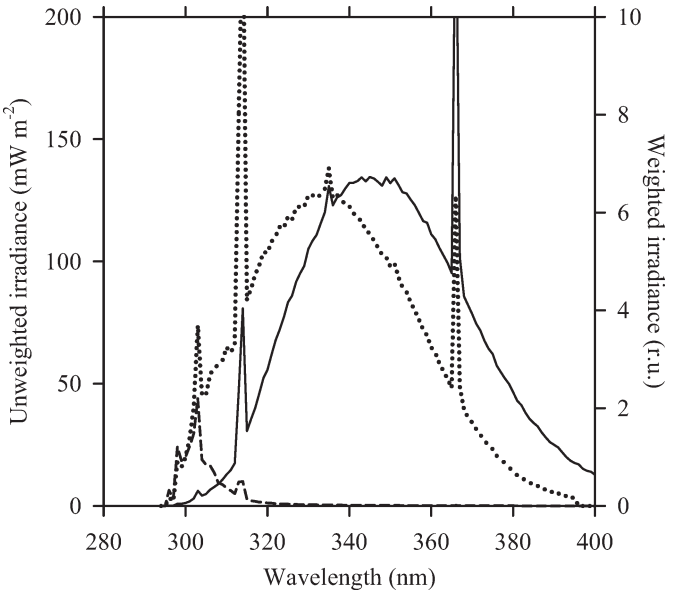

Fig. 1. Spectral irradiance from UVA-340 lamps used to acclimate *T. pseudonana* to UVR exposure in the growth chamber. The solid line shows the unweighted irradiance ($E[\lambda]$, mW m^{-2} nm^{-1}), and the dotted and dashed lines show the weighted irradiance ($E^*_{inh}[\lambda]$, relative units) using the BWF for *Phaeodactylum* photoinhibition (Cullen et al. 1992) and the Setlow action spectra for DNA damage (Setlow 1974), respectively, both normalized at 300 nm for comparative purposes.

values in the growth chamber were measured with a scanning monochromator system (SPG 300 Acton Research, Acton), which uses a 2-π probe with Teflon diffuser, fiber optics, and photomultiplier tube (PMT) detector. Technical details and calibration of the system have been previously described (Neale and Fritz 2001). To calculate the UVR reaching the culture from the UVA-340 lamps (Q-panel), scans were performed with the probe of the spectroradiometer directed horizontally in the position of the Teflon bottle at eight positions covering a 360° angle. The average spectrum was corrected for cellulose acetate and Teflon transmittance spectra, and acceptance angle of the probe (the latter through comparison of the UVA-340 lamps using calculated PAR values in air with the 4-π QSL-2101 measurement in water) to predict scalar spectral irradiance inside the Teflon bottle (Fig. 1). Unweighted irradiance reaching the culture was in the range reported for natural environments (e.g., Neale 2001; Litchman and Neale 2005); values for UVB and UVA were 0.44 W m^{-2} and 6.91 W m^{-2}, respectively. Weighted irradiance calculated using the BWF for the inhibition of photosynthesis in the diatom *Phaeodactylum tricornutum* (Cullen et al. 1992) and the action spectra for DNA damage of Setlow normalized to 300 nm (Setlow 1974) were 0.25 (dimensionless) and 19.19 mW m^{-2}, respectively.

Cellular density and chlorophyll concentration—Cell number was counted every day with a Neubauer hematocytometer. The growth rate (μ, d^{-1}) was calculated as $\ln(N_2/N_1)/t$, where N_1 and N_2 are the cell concentrations on two consecutive days, and t is the time between samples (d). Chlorophyll concentration was measured on aliquots concentrated on glass-fiber filters (GF/F, Whatman Inc.) and extracted with 90% acetone overnight at 4°C. After extraction, the fluorescence emission was measured in a Turner 10-AU fluorometer.

Cellular absorbance—Cellular absorbance of UVR and PAR was analyzed by the quantitative filter technique as described in Cleveland and Weidemann (1993). Cells concentrated on glass-fiber filters (Whatman GF/F) were scanned from 280 to 750 nm in a Cary 4 dual-beam spectrophotometer, using a blank filter wetted with filtrate as a reference. The filter was extracted with 100% methanol, washed with filtrate, and rescanned using a similar procedure as for the nonextracted filter. The absorbance spectrum of the remaining material was subtracted from that from the nonextracted sample before correction for path-length amplification and calculation of the chlorophyll specific cross section ($a^*[\lambda]$, m^2 mg Chl a^{-1}).

Membrane permeability—Changes in membrane permeability were assessed following a modification of the protocol described by Rijstenbil (2005). The assay is based on a lipophilic anion dye ($DIBAC_4$, Molecular Probes), the fluorescence of which depends on membrane potential. The low-fluorescent state corresponds to intact membranes that are polarized (i.e., they maintain a transmembrane electron potential). When membranes are damaged, such that ions can leak across and the membrane is depolarized, fluorescence increases. One microliter of 2 mmol L^{-1} $DIBAC_4$ working solution was added to 1 mL of culture and kept in the dark at 20°C for 30 min. After incubation, cells were washed twice by centrifuging them in a microfuge (14,000 rpm, 1 min) and resuspending the pelleted cells in filtered seawater at 15 salinity, and fluorescence emission was measured at 517 nm in a SPEX FluoroMax-3 spectrofluorometer (excitation 490 nm, bandwidth 5 nm).

Maximum photosynthetic efficiency of PSII—A pulse amplitude–modulated fluorometer Diving PAM/B (Walz) with blue light-emitting-diode (LED; 470 nm) excitation was used to assess the maximum photosynthetic efficiency of the cultures at different times during the experiment. The data are expressed as the photosystem II (PSII) quantum yield, $F_v : F_m = (F_m - F_0) : F_m$, which has been correlated with the maximum quantum yield of photosynthesis (Genty et al. 1989). F_0 is the steady-state yield of in vivo chlorophyll fluorescence in dark-adapted phytoplankton, and F_m is the maximum yield of fluorescence obtained from an illuminated sample after a saturating light pulse (400-ms pulse duration) has been applied.

Photosynthetic responses to PAR and photosynthesis–irradiance (P–E) model—Photosynthesis–irradiance (P–E) curves for PAR-only exposure were obtained in a "photosynthetron" incubator using a modification of the protocol described by Lewis and Smith (1983). The temperature-regulated incubator uses a halogen lamp to assess the photosynthetic response to PAR (n = 24), as the

conversion of inorganic $H^{14}CO_3^-$ (~25 kBq mL^{-1}) into organic compounds during a 1-h incubation. Samples for analysis were collected early in the morning, when chlorophyll concentration was still low (0.3–0.6 μg Chl *a* mL^{-1}), after a standardized inoculation the previous afternoon. Since *T. pseudonana* divides mainly during the light period (Nelson and Brand 1979), collecting the samples in the morning allowed the cells to acclimate to the new media and minimized differences in self-shading and CO_2 demand between high- and low-CO_2 treatments. It is also unlikely that the cultures were synchronized enough that differences in growth rate resulted in a substantial change in the fraction of the population in each stage of the cell cycle for different treatments at the scheduled sample time.

Photosynthetic parameters, P_s^B and E_s, were estimated using nonlinear regression fitting of the equation:

$$P^B = P_s^B \tanh\left(\frac{E_{PAR}}{E_s}\right) \quad (1)$$

where P^B is photosynthesis normalized to Chl *a* content (g C [g Chl a^{-1}] h^{-1}), P_s^B is the maximal rate of photosynthesis, E_s is the saturation irradiance for PAR, and E_{PAR} is the PAR irradiance.

Photosynthetic response to UVR and the threshold model—At the same time, and using similar samples as those used for the photosynthetron incubations, the photosynthetic response to UVR was assessed over 1 h using $H^{14}CO_3^-$ incorporation in a special polychromatic incubator, the "photoinhibitron" (Cullen et al. 1992; Neale 2000; Neale and Fritz 2001). The incubator used a 2,500-W xenon lamp (Solar simulator lamp, Schoeffel Instrument Corp.), which, after appropriate filtration, emits PAR, UVA, and UVB in similar proportions as solar irradiance, allowing the assessment of realistic responses. The beam passed through an array of eight long-pass filters (WG280, WG295, WG305, WG320, WG335, and GG395 [Schott Glass Technologies, Inc.] and LG350 and LG370 [Spectra-Physics], with nominal 50% transmittance [T] at 280, 295, 305, 320, 335, 350, 370, and 395 nm), which were combined with neutral density screens to produce ten irradiances for a total of 80 treatments of varying spectral composition and irradiance. Additional cellulose acetate film (<1% T at less than 288 nm) was also used with the WG320-, WG305-, WG295-, and WG280-nm long-pass filters to eliminate exposure to very short wavelengths. The cellulose acetate was positioned after the long-pass filter in the optical path. The long-pass filters and the cellulose acetate allowed the transmission of wavelengths longer than the cutoff value (e.g., for GG395, $E[\lambda] > 395$ nm), while the neutral density screens reduced irradiance. The light treatments were directed to 1.8-cm-diameter, flat-bottom quartz cuvettes that were mounted within a temperature-regulated block and filled with 1 mL of culture for exposure. Spectral irradiance in each cuvette was measured with the SPG 300 spectroradiometer system.

The BWF/P–E models are based on a PAR-only P–E curve equation, with the addition of a term that represents inhibition of photosynthesis by UVR and PAR and that includes the BWF (Eq. 2). The inhibition term relates the effect of UVR to "weighted" irradiance, E^*_{inh} (i.e., spectral irradiance corrected for the biological effect or "weight"; Eq. 3), and accounts for the kinetics of UVR damage and repair during exposure (Neale 2000). The BWF_T/P–E threshold model (BWF_T/P–E) describes photosynthesis in species for which repair completely compensates for damage, until damage (i.e., E^*_{inh}) reaches a threshold level of 1 (Sobrino et al. 2005). Above the threshold, photosynthesis declines according to the equation:

$$P^B = P_s^B \tanh\left(\frac{E_{PAR}}{E_s}\right) \min\left(1, \frac{1}{E^*_{inh}}\right) \quad (2)$$

$$E^*_{inh} = \sum_{\lambda=280}^{400} \varepsilon(\lambda) E(\lambda) \Delta\lambda + \varepsilon_{PAR} E_{PAR} \quad (3)$$

where min denotes the minimum function, E^*_{inh} is a dimensionless index for the biologically effective or weighted irradiance, and $\varepsilon(\lambda)$ is biological weight ([mW m^{-2}]$^{-1}$) at wavelength λ. $E(\lambda)$ is spectral irradiance (mW m^{-2} nm^{-1}) at λ, and $\Delta\lambda$ is the wavelength resolution, 1 nm. Inhibition by PAR is included using a single broadband weight, ε_{PAR} ([mW m^{-2}]$^{-1}$), for PAR irradiance (Cullen et al. 1992). BWFs were estimated from the measured rates of photosynthesis using nonlinear regression and principal component analysis (PCA) similar to that previously described (Cullen et al. 1992; Neale 2000). The BWFs were calculated for each treatment ($n = 2$), and only two principal components were necessary to explain more than 98% of variance. The BWFs shown in the manuscript correspond to the average BWF for each treatment, where the standard error of the mean (SEM) for each wavelength was calculated from individual error estimates by propagation of errors (Bevington 1969). The degrees of freedom were calculated as the number of points in the photoinhibitron minus the number of fitted parameters (in this case, 80 – 5 = 75).

Assessment of average spectral irradiance in the water column of the Rhode River (1.5-m depth), a turbid estuary on the east coast of the United States, was determined as $E_0(\lambda)(1 - e^{-k(\lambda)z})/k(\lambda)z$, where $E_0(\lambda)$ is incident surface irradiance, $k(\lambda)$ is the attenuation coefficient for a given wavelength, λ, and z is depth (1.5 m). Solar spectra and attenuation coefficients were obtained from Neale (2001). Scalar irradiance in the water column was calculated according to Kirk (1983).

Statistical analysis—Significant differences between treatments were analyzed using a one-way analysis of variance (ANOVA). A Student–Newman–Keuls multiple-comparisons post-test was also applied to indicate where significant differences occurred.

Results

The UVR exposure applied during growth of *T. pseudonana* cultures produced very mild effects on maxi-

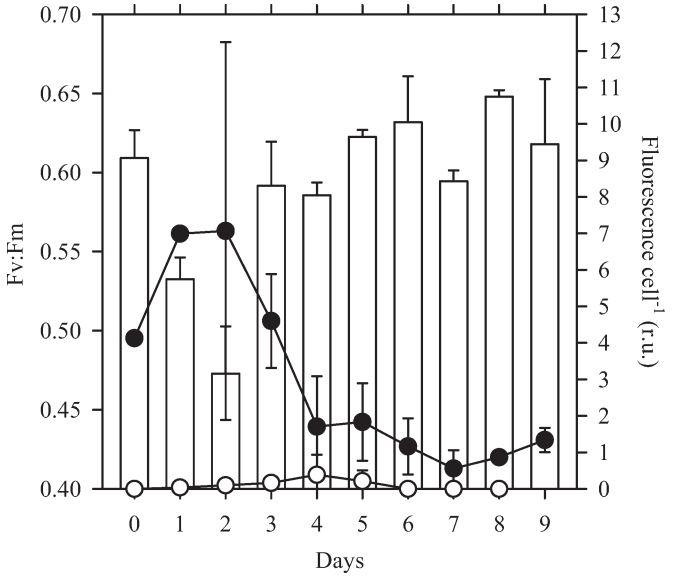

Fig. 2. Changes in photosynthetic efficiency ($F_v : F_m$, bars) and membrane permeability cell^{-1} (i.e., $DIBAC_4$ fluorescence in relative units cell^{-1}, open and closed circles) observed in *T. pseudonana* after transfer from atmospheric to elevated (0.1%) CO_2 concentrations. Open circles indicate membrane permeability in *T. pseudonana* cells grown under atmospheric CO_2 levels, and closed circles correspond to 0.1% CO_2 levels ($n = 2$). Error bars show ranges of duplicates.

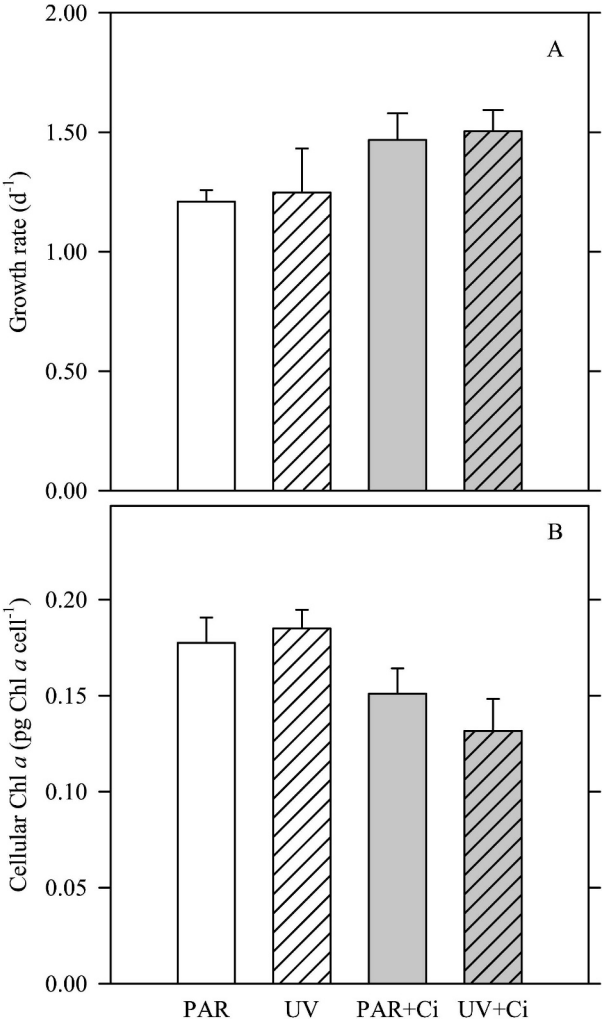

Fig. 3. Growth parameters (mean ± SD, $n = 4$–5) of *T. pseudonana* acclimated to PAR and UVR exposures under atmospheric and elevated (0.1%) CO_2 concentrations. Unshaded bars correspond to low-CO_2 cultures, and shaded bars correspond to high-CO_2 cultures. The presence or absence of hatching inside the bar indicates cultures grown under PAR and PAR + UVR, respectively. (A) Growth rate (d^{-1}) and (B) cellular chlorophyll (pg Chl *a* cell^{-1}).

mum photosynthetic efficiency and growth. The average $F_v : F_m$ ratio was the same (0.60 ± 0.04, $n = 8$) for PAR- and UVR-exposed cells, similar to other $F_v : F_m$ values reported for healthy cells of *T. pseudonana* (Dijkman and Kromkamp 2006). In contrast to the UVR, high CO_2 concentrations produced a 25% decrease in $F_v : F_m$ from day 0 to day 2. Cultures recovered after 3 d of continuous bubbling with 0.1% CO_2 and $F_v : F_m$ values reached similar values as cells grown under atmospheric levels of CO_2 (Fig. 2). The decrease in $F_v : F_m$ under high CO_2 was concomitant with an increase in DIBAC fluorescence (membrane permeability) from day 0 to day 2 and a subsequent decrease during the $F_v : F_m$ recovery. However, membrane permeability in high-CO_2 cells remained slightly higher than in atmospheric CO_2 cultures until the end of the experiment (Fig. 2). Based on the $F_v : F_m$ results, we considered that cells were acclimated to 0.1% CO_2 by day 4. In order to avoid interactions with CO_2 acclimation that might have produced additional effects on *T. pseudonana* metabolism, all the following results were obtained from analysis carried out from day 4.

The results showed that 0.1% CO_2 conditions increased *T. pseudonana* growth rates by 20% ($p = 0.03$, $n = 4$–5) (Fig. 3A); values (mean ± SD) were 1.21 ± 0.05 d^{-1} and 1.21 ± 0.18 d^{-1} for low-CO_2 cultures under PAR and UVR exposures, respectively, and 1.47 ± 0.11 d^{-1} and 1.50 ± 0.09 d^{-1} for the high-CO_2 cultures under similar PAR and UVR exposures. For the same samples, Chl *a* concentrations decreased in the high-CO_2 cultures, resulting in a significant ($p = 0.02$, $n = 4$–5) decrease of 22% in Chl *a* cell^{-1} under the latter conditions (Fig. 3B). Cellular Chl *a* concentrations (mean ± SD) changed from 0.18 ± 0.01 pg Chl *a* cell^{-1} in low-CO_2 cultures grown under PAR and UVR exposures to 0.15 ± 0.01 pg Chl *a* cell^{-1} and 0.13 ± 0.02 pg Chl *a* cell^{-1} in high-CO_2 cultures grown under PAR and UVR, respectively (Fig. 3B). No significant differences in growth rates, Chl *a* concentration, or Chl *a* cell^{-1} were observed between PAR- and UVR-exposed cultures.

Analysis of the Chl *a* specific absorption spectra, $a^*(\lambda)$, demonstrated that CO_2 concentrations also had a major effect on the absorption of short-wavelength irradiance ($\lambda < 500$ nm) by cellular pigments. The $a^*(\lambda)$ value was higher in the high-CO_2 cultures than in the low-CO_2 cultures, and the difference increased with decreasing wavelengths. In contrast, acclimation to UVR during growth did not show clear effects: $a^*(\lambda)$ increased under high CO_2 but decreased under atmospheric CO_2 when compared to PAR-grown

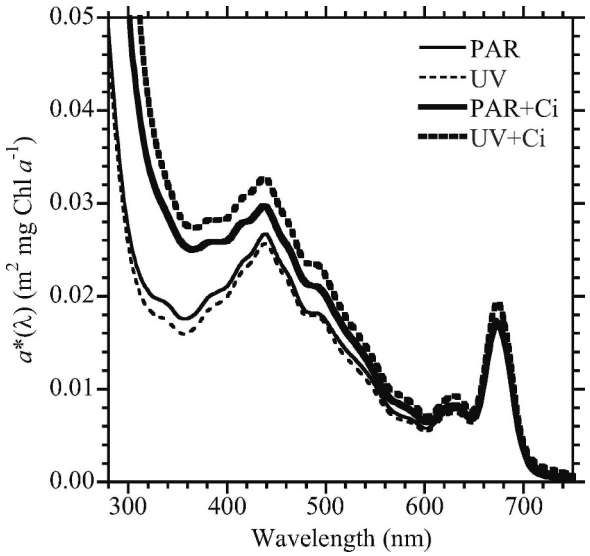

Fig. 4. Cellular absorbance of UVR and PAR measured as Chl *a* specific absorption spectra ($a^*[\lambda]$, m^2 mg Chl a^{-1}) of *T. pseudonana* acclimated to PAR and UVR exposures under atmospheric and elevated (0.1%) CO_2 concentrations ($n = 2$). Thin lines correspond to low-CO_2 cultures, and thick lines correspond to high-CO_2 cultures. The solid lines represent those grown under PAR exposure, and the dashed lines represent those grown under PAR + UVR.

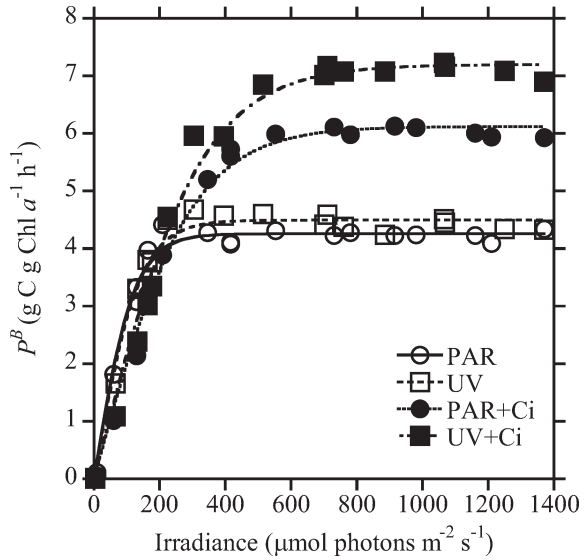

Fig. 5. Photosynthesis–irradiance (P–E) curves for PAR-only exposure of *T. pseudonana* acclimated to PAR and UVR exposures under atmospheric and elevated (0.1%) CO_2 concentrations ($n = 2$). Open symbols correspond to low-CO_2 cultures, and closed symbols correspond to high-CO_2 cultures. The circles represent the cultures grown under PAR conditions, and the squares represent those grown under PAR + UVR. The lines indicate the predicted values using Eq. 1.

cultures (Fig. 4). Despite the increase in $a^*(\lambda)$ observed for all the treatments below 370 nm, no UVR-absorbing compounds have been described for *Thalassiosira*, and it is unlikely that this increase was related to the presence of specific UV-protective compounds such as mycosporine-like amino acids (MAAs). This steep rise in absorbance might have been related to absorbance by nucleic acids, proteins, and other cofactors that were partially removed by the methanol extraction.

Analysis of the P–E curves for each treatment shows that high-CO_2 concentrations increased the maximum rate of photosynthesis and the light saturation parameter (Fig. 5). The effect was independent of light regime during growth, since similar effects were observed between cells grown under PAR or UVR (Fig. 5). The maximal rate of photosynthesis normalized to chlorophyll (P_s^B, g C [g Chl a^{-1}] h^{-1}) increased from 4.25 ± 0.02 and 4.50 ± 0.21 in the low-CO_2 cultures grown under PAR and UVR, respectively, to 5.63 ± 0.64 and 6.62 ± 0.39 in the high-CO_2 cultures. Differences in P_s^B between the low- and high-CO_2 conditions were related to the changes in Chl *a* concentration observed for those treatments, since the maximal rate of carbon fixation normalized by cell number was similar among treatments, with an average of 807.6 ± 87.0 fg C $cell^{-1}$ h^{-1}. In addition, the saturation irradiance parameter (E_s, μmol photons m^{-2} s^{-1}) increased from 126 ± 29 and 139 ± 13 in the low-CO_2 cultures grown under PAR and UVR, respectively, to 297 ± 21.5 and 327 ± 31.5 in the high-CO_2 cultures (Fig. 5).

Exposure of *T. pseudonana* to simulated solar exposures using the Xe-Arc lamp and the photoinhibitron allowed the estimation of biological weighting functions (BWFs) for the inhibition of photosynthesis in cells grown at high and atmospheric CO_2 under PAR and UVR exposures. The strength of the estimation was validated by average values of $R^2 = 0.99$ ($n = 80$), which were obtained by comparing the predicted photosynthetic rates, using the estimated BWFs in the BWF_T/P–E model (Eq. 2), and the observed photosynthetic rates (Fig. 6A) in the exposure response curves (ERCs). The ERCs relate photosynthesis to weighted exposure and comprise the inhibition term of the BWF/P–E model (i.e., $\min[1, \frac{1}{E^*_{inh}}]$ for the BWF_T/P–E model). For comparison, the data were also fit to other BWF/P–E models, such as the BWF_E/P–E model, which applies to cells with repair proportional to damage, and the BWF_H/P–E model, for those with low or insignificant repair (also called T, E, and H models, respectively, for simplicity, as abbreviations for threshold, radiant exposure, and irradiance dependent models, respectively). These fits showed consistently lower R^2 values than those using the T-model. Between the E and H model, the results obtained using the E model were closest to those reported with the T model (e.g., average $R^2 = 0.94$) (Fig. 6B), showing quantitative, more than qualitative, differences among treatments. However, the T model is the more appropriate choice for these cultures, given the systematic bias of the E model fit. The E model tends to underestimate observed rates at moderate exposures while overestimating rates at high exposures (Fig. 6B). In addition, Fig. 7 shows predicted and observed P–E curves (i.e., ERCs for unweighted irradiance) obtained for *T. pseudonana* grown

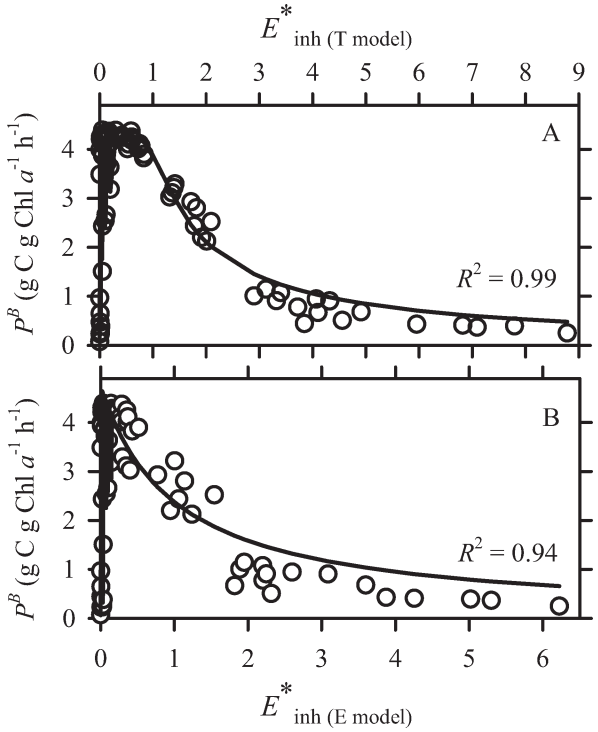

Fig. 6. Exposure response curves (ERCs) of a *T. pseudonana* culture grown under atmospheric levels of CO_2 and PAR + UVR exposures. Open circles are observed photosynthetic rates (g C [g Chl a^{-1}] h^{-1}) obtained during 1-h incubation in the photoinhibitron (n = 80). The solid line shows the predicted rates using "best-fit" parameters for (A) the BWF_T/P–E model (constant repair), and (B) the BWF_E/P–E model (repair proportional to damage). The ordinate axis is weighted irradiance, E^*_{inh}, for the BWF_T/P–E model (upper scale) and for the BWF_E/P–E model (lower scale). The coefficient of determination (R^2) for each fit (n = 80) is also shown.

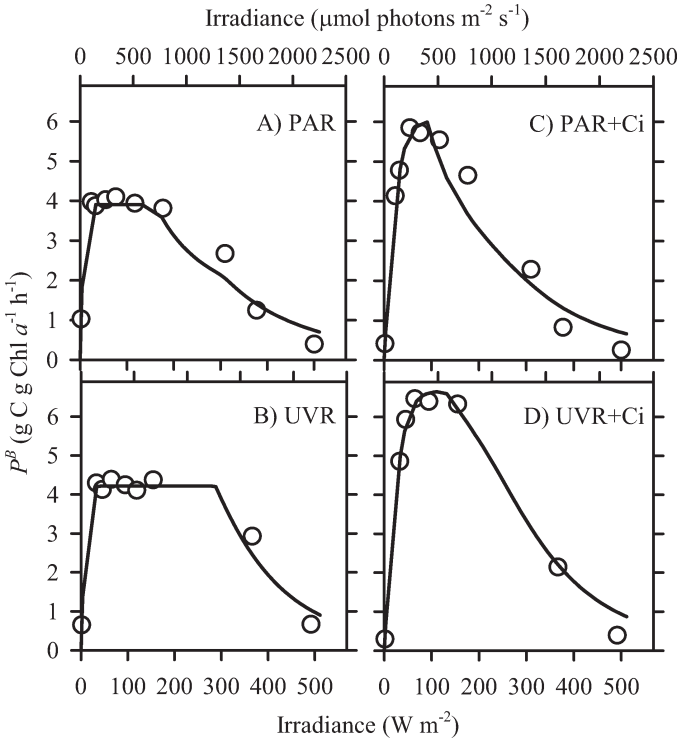

Fig. 7. Photosynthesis–irradiance (P–E) curves (i.e., photosynthetic rates vs. unweighted irradiance) obtained from incubations of *T. pseudonana* in the photoinhibitron (PAR + UVR) using the LG350 long-pass filter (n = 10). The observed rates of photosynthesis (g C [g Chl a^{-1}] h^{-1}) over 1-h exposure using a filtered solar simulator lamp (2,500-W xenon lamp) are indicated by the circles. Exposure conditions in the photoinhibitron differed somewhat in spectral composition between experiments conducted with PAR and UVR cultures, so response should only be compared between atmospheric and elevated (0.1%) CO_2 within each irradiance treatment. The line indicates the predicted values using the fitted BWF_T/P–E model (Eq. 2). PAR irradiance is shown in both μmol photons m^{-2} s^{-1} and W m^{-2} for clarity. (A) PAR, (B) UVR, (C) PAR + Ci, and (D) UVR + Ci.

under elevated and atmospheric CO_2 under PAR and UVR exposures, from incubations in the photoinhibitron using the LG350 long-pass filter (n = 10). The ratio UVR : PAR is relatively constant within this spectral treatment; thus, increased PAR is accompanied by an increase in inhibiting UVR (Fig. 7). The P–E curves also show that high-CO_2 cultures have higher rates at moderate PAR + UVR exposures (e.g., 500 μmol photons m^{-2} s^{-1}) but equal or lower rates at high exposures (e.g., 1,500 μmol photons m^{-2} s^{-1}). They also show high thresholds and soft slopes in photoinhibition at high exposures in cells grown under atmospheric levels of CO_2, especially in cells grown under UVR exposures. In contrast, thresholds are smaller and slopes are sharper under high CO_2, indicating a higher sensitivity to UVR in these cells.

After calculating the effect, or "weight" of exposure ($\varepsilon[\lambda]$, [mW m^{-2}]$^{-1}$), for each spectral treatment in the photoinhibitron, the BWFs demonstrated that sensitivity of photosynthesis to UVR was significantly different between cells grown under elevated and atmospheric CO_2, as well as between cells grown under PAR and UVR exposures (Fig. 8). The $\varepsilon(\lambda)$ values increased in all the BWFs at the shorter, more damaging wavelengths, similar to previously reported BWFs (Fig. 8A,B). Cells grown under elevated CO_2 showed higher sensitivity to UVR than cells grown under atmospheric CO_2, as demonstrated by the higher values in $\varepsilon(\lambda)$. In addition, increased sensitivity under elevated CO_2 concentrations was observed in cells grown under PAR as well as under UVR exposure. Growth under UVR exposure produced opposite effects compared to those under elevated CO_2 conditions. It decreased the sensitivity to UVR, resulting in lower $\varepsilon(\lambda)$ values than the cells grown under PAR (Fig. 8A,B). In all the cases, the significant differences among treatments were mainly observed from 300 to 360 nm, affecting both UVA and UVB regions.

Discussion

This study demonstrates that under saturating light and nutrient conditions, elevated CO_2 concentrations increase growth rates (i.e., cell number) and photosynthesis in *T. pseudonana*. However, the results also showed that the increase in photosynthetic capacity was mainly related to

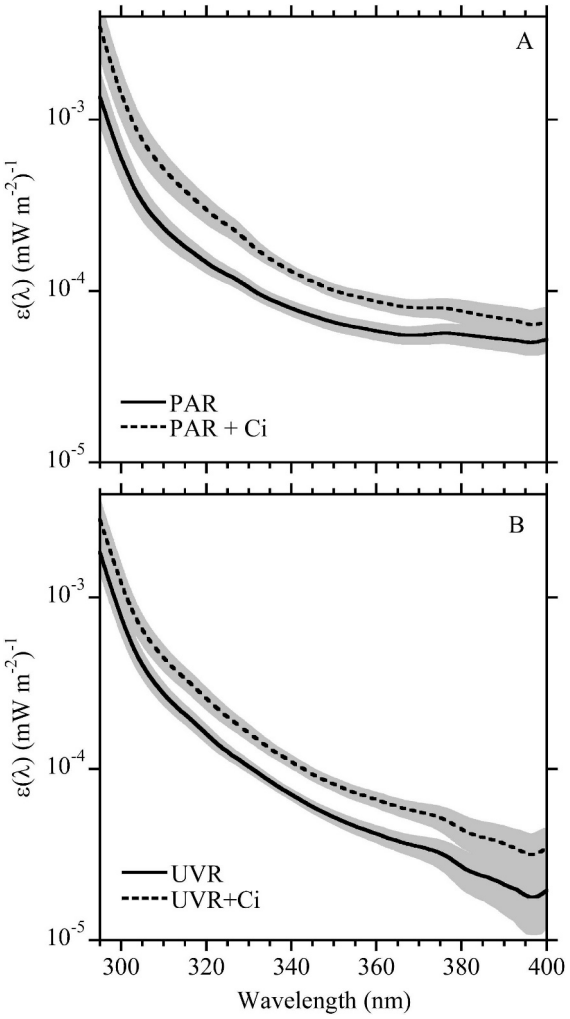

Fig. 8. BWFs for the inhibition of photosynthesis by UVR ($\varepsilon[\lambda]$, [mW m^{-2}]$^{-1}$) of *T. pseudonana* acclimated to PAR and UVR exposures under atmospheric and elevated (0.1%) CO_2 concentrations. Curves are the average BWF (n = 2) for each treatment. The gray shading represents the standard error of the mean (SEM) calculated from error estimates of individual BWFs.

static cellular photosynthesis despite a proportional decrease in cellular chlorophyll, which was an indication of major biochemical and physiological changes in the cells under high-CO_2 conditions. Our results agree with those observed in previous field studies that reported significant effects of CO_2 enrichment on phytoplankton productivity (Hein and Sand-Jensen 1997; Ibelings and Maberly 1998). They partially differ with those from Tortell et al. (2000, 2002), who did not observe significant effects on total biomass, measured as bulk chlorophyll, and primary productivity in Pacific phytoplankton assemblages grown under high- and low-CO_2 concentrations. However, they described active growth and changes in taxonomic composition that favored diatoms against nonsiliceous phytoplankton taxa under high-CO_2 conditions. As stated by the authors of these studies, oceanographic techniques that measure characteristics of entire phytoplankton communities rather than individual taxa may be inadequate to detect potential ecological responses to CO_2 variations. Taking into account the disparity observed in *T. pseudonana* between cell number and chlorophyll content under different CO_2 levels, it is also possible that the changes produced by elevated CO_2 in natural phytoplankton assemblages remain masked when bulk chlorophyll is measured if changes in growth rates are compensated by changes in chlorophyll contents.

Moreover, our results point out the relevance of previous acclimation to elevated CO_2 in evaluations of adapted responses of phytoplankton to new conditions. Changes from low- to high-CO_2 concentrations temporarily affected (i.e., days) *T. pseudonana* metabolism, resulting in increases in membrane permeability and decreases in maximum photosynthetic efficiency. It is likely that growth rates were also depressed during that period of reduced cell performance; however, no data supporting this statement were collected in this study. Some of our previous results have demonstrated that this "short-term" stressing response varies with the CO_2 concentration range and among species with different characteristics of carbon uptake (Sobrino et al. 2005). After 4 d, 1% CO_2 produced a decrease in growth rates and maximum photosynthetic efficiency in *Nannochloropsis gaditana* (HCO_3^- transporter), but no decrease was detected in *Nannochloris atomus* (CO_2 transporter) under similar conditions. Abrupt increases in external CO_2 concentration can temporarily accelerate the activity of the internal carbonic anhydrase (CA_i), the enzyme responsible for converting HCO_3^- to CO_2 in a site close to ribulose-1,5-biphosphate carboxylase-oxygenase (RUBISCO), resulting in the acidification of the stroma and the enhancement of PSI : PSII activity ratios (Satoh et al. 2001). These effects result in a decrease in the photosynthetic efficiency and growth rates, similar to the effects we reported for *Nannochloropsis* and *Thalassiosira*, and they might also be a factor contributing to the membrane depolarization. The effects on phytoplankton metabolism of changes in external pH and ionic balance caused by the increase in CO_2 could have also contributed to the overall response.

After *T. pseudonana* was acclimated to high CO_2 (i.e., recovered to initial $F_v : F_m$ values), cells showed significant changes in the amount and spectral absorption profile of photosynthetic pigments. A high-CO_2 treatment resulted in decreased chlorophyll cell^{-1} and increased chlorophyll-specific absorption cross sections below 500 nm compared to growth under atmospheric CO_2 levels. Similar to the decrease in chlorophyll described for *T. pseudonana*, it has been observed that the expression of CA and RUBISCO and the size of the intracellular pools decrease in phytoplankton after acclimation to elevated CO_2 concentrations (Aizawa and Miyachi 1986; Berman-Frank et al. 1998; Tortell et al. 2000). These responses were related to a down-regulation of the photosynthetic machinery under high CO_2 availability. In addition, cells grown under elevated CO_2 are characterized by significantly higher C : N : P ratios and higher carbohydrate : protein contents (Burkhardt et al. 1999; Tortell et al. 2000). Studies show that the accumulation of internal carbohydrates tends to repress photosynthetic gene transcription (Woodger et al. 2005), resulting in decreased levels of several photosynthetic enzymes related to carbon transport and fixation and

decreased quantum requirements (Berman-Frank et al. 1998; Tortell et al. 2000). Despite the down-regulation of these enzymes, cells can still maintain similar or higher carbon fixation rates, ultimately increasing growth rates, by decreasing the energy cost of photosynthesis and increasing resource-use efficiency (Raven 1991). Likewise in our study, *T. pseudonana* cells assimilated the same amount of carbon under atmospheric and elevated CO_2 concentrations, as demonstrated by the similar rates of carbon assimilation cell^{-1}, but they showed increased efficiency under high CO_2 when carbon rates were normalized to chlorophyll. These results, together with the decreased chlorophyll concentration and increased growth rates under high-CO_2 conditions, suggest a down-regulation of the photosynthetic machinery in *T. pseudonana* as well. However, further analysis (e.g., quantification of RUBISCO or enzymes involved in carbon incorporation) should be carried out to confirm this hypothesis.

The same process that produced the decrease in chlorophyll may also be responsible for the increase in UVR sensitivity observed under elevated CO_2 conditions. Disparity in UVR sensitivity between cells acclimated to elevated and atmospheric CO_2 concentrations was demonstrated in our study by the significant differences observed in the BWFs for the inhibition of photosynthesis (Fig. 7A,B). A down-regulated metabolism shows reduced capability to incorporate and synthesize new metabolites, finally reducing intracellular pools (Aizawa and Miyachi 1986). Tortell et al. (2002) also reported lower N : P and N : Si consumption ratios in natural assemblages incubated at high CO_2. It has been demonstrated that reduced availability of metabolites and nitrogen resources affect the amount and activity of the enzymes involved in cellular repair (Litchman et al. 2002), increasing susceptibility to UVR and resulting in more photoinhibition when UVR stress is imposed than would occur in cells with normal metabolic activity. High-CO_2 cultures might also contain cells with a lower activation state of the general defense mechanism (e.g., lower concentrations cell^{-1} of superoxide dismutase and ascorbate peroxidase), which might be linked to an awareness of the redox state between PSI and PSII (Surpin et al. 2002). Additional analysis of the rates of damage and repair estimated from ΦPSII time series under UVR exposures with a PAM fluorometer, which has been used in previous studies to suggest the mechanism responsible for a change in sensitivity to inhibition (Sobrino et al. 2005), did not provide clarification in the case of elevated CO_2 effects on *T. pseudonana* (data not shown). The changes in ΦPSII with time followed an exponential decrease under UVR exposures that was well explained by equations derived from a constant repair model (average $R^2 = 0.99$) (Sobrino et al. 2005). However, a definitive cause for the differences between cells grown under atmospheric and elevated CO_2 conditions could not be obtained because after acclimation to elevated CO_2, both damage and repair rates changed, probably due to more complex interactions in the cells.

The responses to UVR observed in *T. pseudonana* under atmospheric and elevated CO_2 agree with previous findings that have reported the lack of UVB effect on the carbon incorporation mechanisms (CCMs) of *Dunaliella tertiolecta* (Beardall et al. 2002). It is likely that direct damage of *T. pseudonana* CCMs would contribute to a higher sensitivity to UVR in cells grown under low-CO_2 levels, which have more active CCMs than those grown under high-CO_2 concentrations. Nevertheless, UVB inhibited carbon assimilation in *D. tertiolecta*, resulting in the increase of the internal DIC pool, as measured by the increase in the initial slope of oxygen evolution vs. DIC plots. In contrast, the results from *T. pseudonana* diverge from those observed in *Nannochloropsis*, where growth under 1% CO_2 decreased susceptibility to UVR due to the enhancement of cellular repair for similar rates of damage (Sobrino et al. 2005). The inconsistency seems to be related to the degree of acclimation to elevated CO_2 levels, which is linked to the timing of the BWF determination in relation to the ''short-term'' stressing response. The assessment of the BWFs for the inhibition of photosynthesis in *Nannochloropsis* was carried out after only 4 d growing under 1% CO_2, when cells had just recovered from the stress. This previous stress episode may have enhanced repair capacity. In contrast, *T. pseudonana* was grown under 0.1% CO_2 for 7–10 d before the ^{14}C incubations to obtain the BWFs were started, and it is quite likely that cells were more acclimated to the new conditions. In addition, variation in the experimental design (i.e., 1% CO_2 vs. 0.1% CO_2, growth under low versus high irradiance, etc.) could also be responsible to some extent for those differences.

Acclimation to UVR using the UVA-340 lamp exposure during growth did not change growth rates, chlorophyll content, photosynthetic parameters under PAR, or membrane permeability. However, it reduced the sensitivity of photosynthesis to UVR as shown by the BWFs. UVR irradiance used for this study was into the range observed in nature and close to average irradiances observed in turbid estuaries of the North American east coast, where *T. pseudonana* is common during spring and summer (Table 1). The results differ from those observed in Litchman and Neale (2005), where acclimation to UVR did not produce effects in *T. pseudonana* sensitivity of photosynthesis to UVR. However, differences between both studies can arise from small variations in the light treatment applied during growth of the cells. In that case, cells in the previous study were exposed to lower UVR irradiance than the present study, but they were not protected from the short wavelengths emitted by the UVA-340 lamp by using the cellulose acetate. The higher irradiance from the short wavelengths produced a decrease in growth rates and higher weighted irradiances using the Setlow action spectra for DNA damage than in the present study. In fact, the lack of significant effects on growth and photosynthesis under the UVA-lamp exposure in our study is in accordance with the characteristics that define the threshold model (BWF_T/P–E model, see Material and methods). By definition, photoinhibition is not evident below a threshold of $E^*_{inh} = 1$ (Neale 2000; Sobrino et al. 2005). E^*_{inh} values calculated using the BWFs from this study and the UVA-lamp spectrum resulted in values lower than 1 and therefore should not produce photoinhibition (Table 1). In contrast, predicted rates (using BWF_T/P–E) for exposure to higher irradiances, such as those recorded at the surface at summer midday in the Chesapeake Bay (Neale 2001) showed

Table 1. Weighted irradiance values (E^*_{inh}, dimensionless) and photosynthetic rates (P^B, g C [g Chl a^{-1}] h^{-1}) estimated for *T. pseudonana* acclimated to PAR and UVR + PAR exposures under atmospheric and elevated (0.1%) CO_2 concentrations, using spectral characteristics from different light environments. $E^*_{inh}(Q)$, $E^*_{inh}z$, and $E^*_{inh}(0)$ indicate weighted irradiances for the spectral irradiance in the growth chamber using UVA-340 lamps (Q-panel), for the depth-averaged irradiance in a shallow (1.5 m) turbid estuary at midday in summer, and for the same midday summer spectra at the surface, respectively. P^B_s indicates potential photosynthetic rates in the absence of inhibition (i.e., for any light environment with $E^*_{inh} < 1$), and $P^B(0)$ indicates photosynthetic rates at the surface including the effect of photoinhibition by UVR. % inh (0) shows the percentage inhibition of UV-inhibited photosynthesis relative to potential photosynthesis at the surface.

	$E^*_{inh}(Q)$	$E^*_{inh}z$	$E^*_{inh}(0)$	P^B_s	$P^B(0)$	% inh (0)
PAR	0.60	0.31	3.17	4.25	1.34	68.4
UVR	0.52	0.27	2.47	4.5	1.82	59.6
PAR+Ci	1.03	0.50	5.20	5.63	1.08	80.8
UVR+Ci	0.83	0.37	3.96	6.62	1.67	74.7

that UVR would produce decreases from 60% to 81% in *T. pseudonana* carbon fixation when compared with values in the absence of UVR. Among the cultures in this study, the high-CO_2 cells would be the most inhibited (Table 1). The acclimation to UVR decreased the susceptibility to UVR by 10%, while the acclimation to 0.1% CO_2 increased susceptibility to UVR by 38%. Based on these results, the incremental effect of increased UVB due to ozone depletion is small compared to the incremental effect of increased CO_2 on increasing sensitivity (Neale 2001). Also, increases in UVB due to ozone depletion are probably too small to increase further acclimation. A more fundamental question is the extent to which increased sensitivity to UVR counteracts increased productivity on a water-column basis. Based on the responses of cultures used in the present study, UVR photoinhibition would extend to the first 10 (low CO_2) to 20 (high CO_2) cm of the 1.5-m water column in the Rhode River Estuary (Fig. 9). Higher carbon fixation at mid-depth

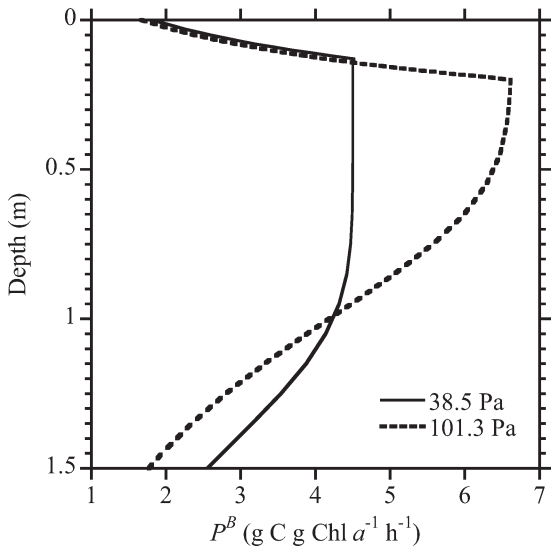

Fig. 9. Vertical profiles of P^B (g C [g Chl a^{-1}] h^{-1}) estimated for the Rhode River (1.5-m depth), a turbid estuary on the east coast of the United States, using a summer midday solar irradiance spectrum and average spectral attenuation from Neale (2001), and average BWFs for the inhibition of photosynthesis in *T. pseudonana* acclimated to atmospheric and elevated (0.1%) CO_2 concentrations under UVR exposures.

carried out under elevated CO_2 conditions would compensate for the increased susceptibility to UVR in the near-surface zone and the lower performance when light becomes limiting (Fig. 9). For this particular case, elevated CO_2 would still enhance water-column productivity by 14% despite the increase in UVR susceptibility and decrease in photosynthesis at depth. This is not intended as a general prediction, only as an illustration that the responses we measured imply significant tradeoffs in water-column responses. The comparison could be substantially different in aquatic systems with higher UVR transparency, in which inhibition extends deeper. In addition, the results are based on the use of only one species of diatom, and we should be cautious when extrapolating the results obtained in this study.

In conclusion, the results showed that elevated CO_2 concentrations significantly affected the photosynthetic metabolism in *T. pseudonana* by reducing chlorophyll content and increasing the chlorophyll specific cross section, the carbon fixation per chlorophyll, and finally, the growth rates. However, cells acclimated to elevated CO_2 were more sensitive than those under atmospheric CO_2 levels when they were exposed to photoinhibitory UVR. In addition, the results demonstrated that the susceptibility to UVR also depended on the previous light history (i.e., UVR regime). Pre-exposure to UVR enhanced UVR acclimation and reduced the sensitivity to photoinhibitory exposures, counteracting, to some extent, the increase in susceptibility observed under elevated CO_2. These interactions will all contribute to the ultimate effect of higher CO_2 on aquatic phytoplankton productivity.

References

Aizawa, K., and S. Miyachi. 1986. Carbonic anhydrase and CO_2 concentrating mechanisms in microalgae and cyanobacteria. FEMS Microbiol. Rev. **39:** 215–233.

Armbrust, E. V., and others. 2004. The genome of the diatom *Thalassiosira pseudonana*: ecology, evolution, and metabolism. Science **306:** 79–86.

Banaszak, A. T., and P. J. Neale. 2001. UV sensitivity of photosynthesis in phytoplankton from an estuarine environment. Limnol. Oceanogr. **46:** 592–600.

Beardall, J., P. Heraud, S. Roberts, K. Shelly, and S. Stojkovic. 2002. Effects of UV-B radiation on inorganic carbon acquisition by the marine microalga Dunaliella tertiolecta (Chlorophyceae). Phycologia **41:** 268–272.

Berman-Frank, I., J. Erez, and A. Kaplan. 1998. Changes in inorganic carbon uptake during the progression of a dinoflagellate bloom in a lake ecosystem. Can. J. Bot. **76:** 1043–1051.

Bevington, P. R. 1969. Data reduction and error analysis for the physical sciences., McGraw-Hill.

Boucher, N. P., and B. B. Prézelin. 1996. Spectral modeling of UV inhibition of *in situ* Antarctic primary production using a newly derived biological weighting function. Photochem. Photobiol. **6:** 407–418.

Burkhardt, S., I. Zondervan, and U. Riebesell. 1999. Effect of CO_2 concentration on C : N : P ratio in marine phytoplankton: A species comparison. Limnol. Oceanogr. **44:** 683–690.

Cleveland, J. S., and A. D. Weidemann. 1993. Quantifying absorption by aquatic particles: A multiple scattering correction for glass-fiber filters. Limnol. Oceanogr. **38:** 1321–1327.

Cullen, J. J., P. J. Neale, and M. P. Lesser. 1992. Biological weighting function for the inhibition of phytoplankton photosynthesis by UV radiation. Science **258:** 646–650.

Dijkman, N. A., and J. J. Kromkamp. 2006. Photosynthetic characteristics of the phytoplankton in the Scheldt estuary: Community and single-cell fluorescence measurements. Eur. J. Phycol. **41:** 425–434.

Elzenga, J. T., H. B. A. Prins, and J. Stefels. 2000. The role of extracellular carbonic anhydrase activity in inorganic carbon utilization in *Phaeocystis globosa* (Prymnesiophyceae): A comparison with other marine algae using the isotope disequilibrium technique. Limnol. Oceanogr. **45:** 372–380.

Gala, W. R., and J. P. Giesy. 1991. Effects of ultraviolet radiation on the primary productivity of natural phytoplankton assemblages in Lake Michigan. Ecotoxicol. Environ. Safety **22:** 345–361.

Genty, B., J. M. Briantais, and M. R. Baker. 1989. The relationship between the quantum yield of photosynthetic electron transport and quenching of chlorophyll fluorescence. Biochim. Biophys. Acta. **990:** 87–92.

Granum, E., J. A. Raven, and R. C. Leegood. 2005. How do marine diatoms fix 10 billion tones of inorganic carbon per year? Can. J. Bot. **83:** 898–908.

Hein, M., and K. Sand-Jensen. 1997. CO_2 increases oceanic primary production. Nature **388:** 526–527.

Hessen, D. O., E. Van Donk, and T. Andersen. 1995. Growth responses, P-uptake and loss of flagellae in *Chlamydomonas reinhardtii* exposed to UV-B. J. Plankton Res. **17:** 17–27.

Ibelings, B. W., and S. C. Maberly. 1998. Photoinhibition and the availability of inorganic carbon restrict photosynthesis by surface blooms of cyanobacteria. Limnol. Oceanogr. **43:** 408–419.

IPCC (Intergovernmental Panel on Climate Change). 2001. Climate change 2001: The scientific basis. Cambridge Univ. Press.

Kirk, J. T. O. 1983. Light and photosynthesis in aquatic ecosystems, 2nd ed. Cambridge Univ. Press.

Leavitt, P. R., B. F. Cumming, J. P. Smol, M. Reasoner, R. Pienitz, and D. A. Hodgson. 2003. Climatic control of ultraviolet radiation effects on lakes. Limnol. Oceanogr. **48:** 2062–2069.

Leonardos, N., and R. J. Geider. 2005. Elevated atmospheric CO_2 increases organic carbon fixation by *Emiliana huxleyi* (Haptophyta), under nutrient-limited high light conditions. J. Phycol. **41:** 1196–1203.

Lewis, M. R., and J. C. Smith. 1983. A small volume, short incubation-time method for measurement of photosynthesis as a function of incident irradiance. Mar. Ecol. Prog. Ser. **13:** 99–102.

Litchman, E., and P. J. Neale. 2005. UV effects on photosynthesis, growth and acclimation of an estuarine diatom and cryptomonad. Mar. Ecol. Prog. Ser. **300:** 53–62.

———, P. J. Neale, and A. T. Banaszak. 2002. Increased sensitivity to ultraviolet radiation in nitrogen-limited dinoflagellates: Photoprotection and repair. Limnol. Oceanogr. **47:** 86–94.

Murphy, T. M. 1983. Membranes as targets of ultraviolet radiation. Physiol. Plant. **58:** 381–388.

Neale, P. J. 2000. Spectral weighting functions for quantifying the effects of UV radiation in marine ecosystems, p. 72–100. *In* S. J. de Mora, S. Demers and M. Vernet [eds.], The effects of UV radiation on marine ecosystems. Cambridge Univ. Press.

———. 2001. Modeling the effects of UV radiation on estuarine phytoplankton production: Impact of variations in exposure and sensitivity to inhibition. J. Photochem. Photobiol. B: Biol. **62:** 1–8.

———, R. F. Davis, and J. J. Cullen. 1998. Interactive effects of ozone depletion and vertical mixing on photosynthesis of Antarctic phytoplankton. Nature **392:** 585–589.

———, and J. J. Fritz. 2001. Experimental exposure of plankton suspensions to polychromatic UV radiation for determination of spectral weighting functions, p. 291–296. *In* J. Slusser, J. R. Herman and W. Gao [eds.], UV Ground- and Space-based Measurements, Models, and Effects. SPIE (The International Society for Optical Engineering).

Nelson, D. M., and L. E. Brand. 1979. Cell division periodicity in 13 species of marine phytoplankton on a light : dark cycle 1. J. Phycol. **15:** 67–75.

———, P. Treguer, M. A. Brzezinski, A. Leynaert, and B. Queguiner. 1995. Production and dissolution of biogenic silica in the ocean: Revised global estimates, comparison with regional data and relationship to biogenic sedimentation. Glob. Biogeochem. Cy. **9:** 359–372.

Raven, J. A. 1991. Physiology of inorganic C acquisition and implications for resource use efficiency by marine phytoplankton: Relation to increased CO_2 and temperature. Plant Cell Environ. **14:** 779–794.

———. 1997. Putting the C in phycology. Eur J. Phycol. **32:** 319–333.

Reinfelder, J. R., A. M. L. Kraepiel, and F. M. M. Morel. 2000. Unicellular C_4 photosynthesis in a marine diatom. Nature **407:** 996–999.

Riebesell, U., D. A. Wolf-Gladrow, and V. Smetacek. 1993. Carbon dioxide limitation of marine phytoplankton growth rates. Nature **361:** 249–251.

Rijstenbil, J. W. 2005. UV- and salinity-induced oxidative effects in the marine diatom *Cylindrotheca closterium* during simulated emersion. Mar. Biol. **147:** 1063–1073.

Sabine, C. L., and others. 2004. The oceanic sink for anthropogenic CO_2. Science **305:** 367–371.

Satoh, A., N. Kurano, and S. Miyachi. 2001. Inhibition of photosynthesis by intracellular carbonic anhydrase in microalgae under excess concentrations of CO_2. Photosynth. Res. **68:** 215–224.

Setlow, R. B. 1974. The wavelengths in sunlight effective in producing skin cancer: A theoretical analysis. Proc. Natl. Acad. Sci. USA **81:** 3363–3366.

Sobrino, C., O. Montero, and L. M. Lubian. 2004. UV-B radiation increases cell permeability and damages nitrogen incorporation mechanisms in *Nannochloropsis gaditana*. Aquat. Sci. **66:** 421–429.

———, P. J. Neale, and L. M. Lubian. 2005. Interaction of UV radiation and inorganic carbon supply in the inhibition of photosynthesis: Spectral and temporal responses of two marine picoplankters. Photochem. Photobiol. **81:** 384–393.

SURPIN, M., R. M. LARKIN, AND J. CHORY. 2002. Signal transduction between the chloroplast and the nucleus. Plant Cell **14:** 327–338.

TORTELL, P. D., AND F. M. M. MOREL. 2002. Sources of inorganic carbon for phytoplankton in the eastern subtropical and equatorial Pacific Ocean. Limnol. Oceanogr. **47:** 1012–1022.

———, G. H. RAU, AND F. M. M. MOREL. 2000. Inorganic carbon acquisition in coastal Pacific phytoplankton communities. Limnol. Oceanogr. **45:** 1485–1500.

VILLAFAÑE, V. E., A. G. J. BUMA, P. BOELEN, AND E. W. HELBLING. 2004. Solar UVR-induced DNA damage and inhibition of photosynthesis in phytoplankton from Andean lakes of Argentina. Arch. Hydrobiol. **161:** 245–266.

VINCENT, W. F., AND P. J. NEALE. 2000. Mechanisms of UV damage to aquatic organisms, p. 149–176. *In* S. J. de Mora, S. Demers and M. Vernet [eds.], The effects of UV radiation on marine ecosystems. Cambridge Univ. Press.

WEATHERHEAD, E. C., AND S. B. ANDERSEN. 2006. The search for signs of recovery of the ozone layer. Nature **441:** 39–44.

WILLIAMSON, R., AND T. PLATT. 1991. Ocean biogeochemistry and air–sea CO_2 exchange. Int. Geosphere-Biosphere Prog. Newslett. **6:** 3–4.

WOODGER, F. J., M. R. BADGERAND, AND G. D. PRICE. 2005. Regulation of cyanobacterial CO_2-concentrating mechanisms through transcriptional induction of high-affinity Ci-transport systems. Can. J. Bot. **83:** 698–710.

Received: 28 May 2007
Accepted: 9 September 2007
Amended: 16 October 2007